A Tunable X-ray Interferometer and the Empirical Determination of Phases Diffracted X-rays

Hong-Yee Chiu

NASA Goddard Institute for Space Studies
Goddard Space Flight Center
New York, New York 10025

Celia C. Chiu

St. lukes Hospital Center
New York, New York 10025

In this paper we present a scheme of X-ray interferometry. The most important feature of this proposed interferometer is the generation of two coherent beams that intersect at continuously variable angles. This is achieved by the application of the Borrmann effect and Bragg reflection in per crystals. The narrow bandwidth of the transmission window of the Borrmann effect allows the use of conventional X-ray generators as X-ray sources with a coherence length between 10μ and 100μ for the interfering beams. A diffraction scheme, similar to certain n-beam cases, is proposed to obtain simultaneous diffractions of these two coherent beams into a common direction. A change in intensity caused by interference will yield the relative phase between these simultaneously diffracted beams. Technological feasibilities are discussed.

I. Introduction.

In the application to the study of organic crystal structures, the central problem in X-ray diffraction is the determination of the phases of the diffracted rays. Except for certain n-beam cases in perfect crystals,[1] the solution of structure depends on various indirect techniques such as the statistical, heavy atom, and multiple isomorphous replacement methods.[2] Although significant results have been obtained with these methods for certain materials, there are certain classes of molecules such as hormones, for which little success has been achieved in structural determination because the appropriate phase information is lacking.

Successful operations of X-ray interferometers and its recent extension to neutron cases have been reported.[3,4] Their success pointed out the important fact that coherent X-ray beams can indeed be generated from conventional X-ray sources to produce interference. Based on the interferometer principle, we propose in this paper an "interfero-diffractometer" to generate two coherent beams capable of producing first order interference for measurements of relative phases of diffracted X-rays. In our subsequent discussions we can and will neglect all anomalous effects of transmission, absorption and serial reflections inside the sample under study. The omission of these phenomena from our subsequent discussion of phase determination is justified if the crystal is ideally imperfect. Thus, only classical interference phenomena will be discussed, together with a strictly kinematical theory of X-ray diffraction.

In Section II we show that by using mirror reflections alone, it is not possible to construct an interferometer generating two coherent beams intersecting at arbitrary angles. On the other hand, it is also demonstrated that, by introducing beam path correctors based on the Borrmann effect,[5] it is possible to design an interferometer that will produce intersecting beams with a variable angle of intersection. The coherence of the intersecting beams also is discussed.

In Section III a general scheme is presented to determine phase differences of the diffracted X-rays from a sample. In Section IV we discuss the feasibility of our interfero-diffractometer. Although in this paper we will not describe the detailed technical problems associated with the actual construction of the interferometer, from studies of dimensional stabilities as well as techniques developed for monitoring dimensional changes to a small fraction of an Ångstrom, our tentative conclusion is that the proposed interferometer can be built within existing technology. Further, it is our conclusion that interfero-diffractometers would be the first appropriate step towards solving the phase determination problem even if X-ray lasers were available. (Of course, the availability of an X-ray laser could certainly improve beam intensity and increase photon correlation lengths.)

II. Generation of Coherent Beams.

(i) Statement of the Problem.

In order to determine the phase relationships between diffracted rays from mosaic crystals, as will be shown later, it is necessary to have a pair of coherent, intersecting beams at the sample point and the angle between the two intersecting beams must fulfill diffraction conditions. These pairs of intersecting beams must be generated from a single source. From the principle of superposition, photons from two separate sources do not interact in the lowest order and consequently do not interfere. In addition, at all intersecting points the phase differences between all pairs of beams originating from their respective source points must be the same, otherwise the interference phenomenon will be averaged out.

Two types of reflection mechanisms exist for X-rays, the glancing angle of incidence reflection and Bragg reflection. In the case of glancing angle of incidence reflection, X-rays of wavelength λ are reflected from a medium with an electron density n_e, provided the angle of incidence θ_i is less than the critical angle θ_{cr} given by :

$$\theta_{cr} \cong \sqrt{\frac{n_e e^2 \lambda^2}{\pi m c^2}} \cong \sqrt{5.4 \times 10^{-5} \frac{n_e}{10^{24}}} \frac{\lambda}{\text{Å}} \text{ radians} \qquad (1)$$

where all symbols have their usual meanings, and c.g.s. and Gaussian units will be used throughout this paper. For X-rays of the relevant wavelengths (0.5 Å to 2.5 Å), θ_{cr} is usually small ($\theta_{cr} \sim 0.4^{o}$ at $n_e \sim 10^{24}$ and $\sim$ 1 Å), In addition, in each reflection a sizable fraction of the incident rays is absorbed, making tandem reflections an impractical method to achieve large angle reflections. In the case of Bragg reflection, the incident angle is fixed by crystal parameters and by the wavelength of interest. The efficiency of reflection, however, can be quite high. For strictly monochromatic X-rays, reflection coefficient can be greater than 90 % when perfect crystals are used.[5]

Up to now, in the X-ray regime, there is only one practical way to achieve beam splitting, namely through the Borrmann effect in a perfect crystal.[5] The entrance and exit surfaces of a perfect crystal make a non-zero angle with the lattice plane for Laue diffraction. When the incident beam is close to satisfying the Laue diffraction condition, wavefields are set up along the lattice. At the exit surface, the wavefield is split into two beams with equal intensities, both making the Bragg angle with the lattice planes and propagating in two separate directions. Absorption inside the crystal is anomalously low; the amount absorbed depends on the particular set of lattice planes used, the amount of dislocations, and other effects.[5] (Figure 1.) The components of the emerged rays that are perpendicular to the lattice planes are well collimated, with a typical angular divergence of the order of seconds of arc, and a band-

width of $\Delta\lambda/\lambda \sim 10^{-5}$.

Utilizing the Borrmann effect for beam splitting and Bragg reflection, the problem of generating two coherent X-ray beams from a single source via interferometer techniques is subject to two restrictions:

(1a) Angles of incidences of all reflecting planes are dictated by appropriate diffraction conditions associated with available and useful crystal planes;

(1b) Angles between splitted beams are dictated by the same restrictions as in (1a).

In addition, the following interferometer conditions must be fulfilled:

(2a) A pair of beams originating from the same source point must intersect later;

(2b) The phase difference between two beams within a pair must be the same for all pairs at their respective intersection points.

Then, to be of practical value, it is necessary that:

(2c) The angle of intersection must be continuously variable over a useful range.

Optical configurations satisfying (2a) through (2c) under restrictions (1a) and (1b) will be hereafter referred to as interfero-diffractometers.

(ii) Impossible configurations.

Bonse and Hart have successfully constructed several Michaelson-type interferometers.[1] In interferometers of this type, conditions (2a) and (2b) are fulfilled. In addition, the path lengths of individual rays from a source point to its intersection point are

the same for all possible source points. It appears natural to extend their principle to cases where the intersection angle can be varied.

We now show that by using reflecting surfaces only, it is not generally possible to fulfill all conditions (2a), (2b), and (2c) simultaneously, under restrictions (1a) and (1b). Each reflection surface has two degrees of freedom in orientation (the distance between reflection surfaces to beam splitting points determines the dimension of the system). In order to bring a pair of beams from a beam splitting point to an intersection point, keeping (2b) and (2c) in mind, at least two reflection surfaces must be used. Altogether there are four degrees of freedom for the two reflection surfaces used. Two of these four degrees of freedom are used to satisfy the incidence angle restriction (1a). Because of the plane geometrical configuration, the condition of intersection (2a) must be fulfilled for three pairs of rays originating from three non-colinear source points. This requires three degrees of freedom whereas only two exist. No new degrees of freedom are introduced by adding more reflection surfaces, since rays emerging from the new surfaces are related to the rays from previous surfaces via reflection laws under the same restrictions (1a) and (1b). If condition (2c) is relaxed, the resulting instrument is a Bonse and Hart interferometer.

(iii) A possible interfero-diffractometer configuration.

C. C. Chiu showed that it is possible, under certain conditions, to construct an interfero-diffractometer.[6] One possible configuration is shown in Figure 2.

A single perfect crystal is carved into an L-shaped slab, such

that one side R is parallel and the other T is perpendicular to a selected set of lattice planes LP. The T side is used to split an incident beam I into two beams I_1 and I_2 via the Borrmann effect, and the angular separation of I_1 and I_2 is 2 θ where θ is the Bragg angle for the selected set of lattice planes. Upon reflection from LP on the R side of the slab, I_1 changes its direction by 2 θ to become I_1' which is now parallel to I_2. (Figure 2). It should be noted that as long as there is no strain in the crystal, the X-rays transmitted through a perfect crystal via the Borrmann effect are always in phase even if the surface is not smooth on the atomic scale. The haggard surface will produce differences in path lengths, but in integer number of wavelengths. Thus the splitted beams can be recombined and interference observed as long as the difference in path lengths does not exceed the correlation length of the photon. The same argument applies for the reflection of X-rays by a perfect crystal. The successful construction of both Laue and Bragg type interferometers by Bonse and Hart clearly demonstrated this point. However, in our proposed scheme of mixed transmission and reflection, there is a systematic and source position dependent path length difference between I_2 and I_1' (Figure 2). If the splitted beams exited at t from the intersection of T and R, then at a plane perpendicular to I_1' and I_2, the systematic path length difference between I_2 and I_1' is 2 t sin θ. Therefore, for any reasonable values of θ, this difference in path lengths will exceed the correlation length of the photon. In order to compensate for this systematic changes in path length, two Borrmann transmission wedges are inserted into the

path of I_2. After transmission through the wedges, I_2 emerges as I_2' such that I_2 and I_2' are colinear. The geometry of the two wedges is determined by (a) the Borrmann transmission condition (essentially the Bragg condition), (b) the elimination of source position dependence of the phase differences between I_2' and I_1' at a plane perpendicular to both I_2' and I_1', and (c) I_2 and I_2' are colinear (in order to preserve the original beam configuration). The two wedges are mirror images of each other; the wedge angle is η and the surface of one side of the wedge makes an angle $\pi/2 - \theta' + \eta$ with the Borrmann transmission lattice plane (thus the other side of the wedge is perpendicular to I_2 or I_2'). θ' is the Bragg angle of the Borrmann transmission plane of the wedge. The complete configuration is shown in Figure 2.

Using conditions (a), (b), and (c), and neglecting, for the time being, the effect of the refractive index of the crystals in optical path calculations, a straightforward evaluation gives the wedge angle η :

$$\tan\eta = \frac{\sin\theta\cos\theta'}{\cos\theta(1-\cos\theta')} \qquad (2)$$

Note that the dimension of the wedge is absent in the determination of η . In order to make the path lengths of I_1 and I_2 equal, additional path extenders using multiple reflections can be inserted.

Because of absorption inside the wedges, the intensity distribution will also be source position dependent. If the source point is at a distance t from the R side of the ...

slab and the width of the source is Δt, the amount to be corrected for in path length over the entire range of Δt is $2\Delta t \sin\theta$. Path correction requires an additional transmission through a thickness of $2\Delta t \sin\theta$ in a perfect crystal so that at the two extremes of Δt the ratio of intensities is 1: $\exp -\mu(2\Delta t \sin\theta)$ where μ is the absorption coefficient. For the σ polarization of the α branch[3] (the strongest transmitted component), $\mu = \mu_o(1-\epsilon)$ where μ_o is the mass absorption coefficient without taking into account of anomalous transmission and ϵ is a correction factor for anomalous transmission (Borrmann effect). ϵ depends on the particular set of lattice planes used as well as on the geometry. Using the example cited by Batterman and Cole[3], for $\Delta t = 0.5$ mm (500μ) and $2\theta = 45^o$ (Ge 220 at Cu Kα), $\mu_o = 350\ cm^{-1}$, $\epsilon = 0.95$, the ratio of intensities is $1 : \exp -1.9 \sin(22.5^o) \cong 1 : e^{-0.7}$. This can be taken into account by an appropriately shaped absorber, as will be discussed in Sect. IV.

I_1' and I_2' then fall onto two mirrors M_1 and M_2 respectively. The surfaces of M_1 and M_2 are parallel to a selected set of lattice planes and M_1 and M_2 are mounted in such a way that their orientations can be rotated about the directions of I_1' and I_2' respectively. By suitable orientation of the two mirrors it is possible to bring the two reflected rays R_1 and R_2 to intersect at a point T. Because of the mirror symmetry between corresponding rays of I_1' and I_2' from different source points, it is easily seen that all rays irrespective of source point positions will intersect. This is the case even though, due to refractive index

corrections, the beam I_1, reflected by the slab LP, is not exactly parallel to I_2, as long as a mirror symmetry is preserved. Although the path lengths of individual rays are different, the path difference between pairs of intersecting rays originating from the same source point can be made to be theoretically zero. The angle of intersection, δ, is a function of the two mirror angles ϕ, which is the angle of the normal to the reflecting plane with respect to the plane defined by I_1' and I_2'. We have:

$$\cos\delta = \cos^2 2\theta_m - \sin^2 2\theta_m \cos 2\phi \qquad (3)$$

where θ_m is the Bragg angle for M_1 and M_2. The range of δ is between 0 and 4 θ_m. With $\lambda = 1.54$ Å (Cu Kα), $\theta_m \sim 45^\circ$ for Ge (333) plane. Thus by suitable choice of reflecting planes it is possible to cover virtually all angles between $\delta = 0^\circ$ and 180°.

(iv). Useful X-ray Sources.

In the interferometer discussed in (iii), the path difference between pairs of intersecting beams originating from the same source point is theoretically zero, so that in principle, the interference condition is always fulfilled. However, practical considerations limit the interference zone roughly to the photon correlation length $\Delta\ell$,

$$\Delta\ell = \lambda^2/\Delta\lambda \qquad (4)$$

Here $\Delta\lambda$ is the spectral bandwidth of I_1' and I_2'. For raw line radiation from conventional X-ray generators, $\Delta\lambda/\lambda \sim 10^{-3}$, and $\Delta\ell \sim 0.2\mu$. However, due to the Borrmann effect, the transmitted beams will have substantially lower bandwidths. The transmitted bandwidths can be estimated from the Bragg condition;

$$\Delta\lambda/\lambda \sim \left(\cos\theta/\sin\theta\right)\Delta\theta \qquad (5)$$

where $\Delta\theta$ is the angular divergence of the transmitted beam, usually a few seconds of arc. Thus $\Delta\ell \sim 30\mu/\Delta\theta(\text{sec})$. Bonse and Hart utilized multiple reflections to obtain a tail-less narrow band filter of angular width $\sim$2 seconds of arc.[7] By using two multiple reflection filters in tandem, it is possible to further reduce the bandwidth. Needless to say, the availability of an X-ray laser will greatly simplify the X-ray source problem. However, the availability of a laser is not absolutely necessary to generate two coherent beams for interferometer application, as already demonstrated by Bonse and Hart.[3]

Line radiation from Mössbauer nuclei would provide a very useful X-ray source. However, it may be difficult to obtain a collimated beam with a sufficient intensity for diffraction work.[8] A new source of intense X-rays is the synchrotron radiation from electron accelerators. Generally, synchrotron radiation when applied to X-ray diffraction work will give a useable collimated beam of intensities roughly 2,000 to 50,000 stronger than that from an ordinary X-ray generator.[9] This may prove to be adequate for the proposed interfero-diffractometer. This topic will be further discussed in Section IV.

III. Phase Determination.

Assuming that two coherent beams intersect at a point T, we now discuss the procedure of extracting phase information from diffracted X-rays. The geometry of X-ray diffraction is described in terms of reciprocal lattices and the Ewald sphere of reflection. Figure 3 depicts the proper condition for diffraction to take place; $\underset{\sim}{H}$ is a vector normal to the reflecting plane and its magnitude is the reciprocal of the interplanar distance. The Ewald sphere, of radius $1/\lambda$, center T, has the origin of the reciprocal lattice O at the end of a diameter which coincides with the direction of the incident ray, TO. The diffracted ray TP intersects $\underset{\sim}{H}$ and the sphere at a point P($\underset{\sim}{H}$), and the diffraction condition is fulfilled with the Bragg condition in reciprocal form:

$$(1/\lambda)\sin\theta_B = (1/2)\underset{\sim}{H} \qquad (6)$$

The diffracted ray is detected in the direction TP. The time independent component of the expression of the wave for the diffracted beam, F($\underset{\sim}{H}$), is determined by the structure within the unit cell of the crystal, and is generally represented by

$$F(\underset{\sim}{H}) = \sum_{n=1}^{N} f_n \exp 2\pi i (\underset{\sim}{r}_n \cdot \underset{\sim}{H}) = \int_V \rho(\underset{\sim}{r}) \exp 2\pi i (\underset{\sim}{r} \cdot \underset{\sim}{H}) dV \qquad (7)$$

where $\rho(r)$ is the electron density at r measured from T, f_n is the scattering factor of the n^{th} atom appropriately corrected for the simultaneous presence of both beams and r_n the vector for its location in the unit cell. F($\underset{\sim}{H}$) is a complex

quantity given by:

$$F(\underset{\sim}{H}) = \left|F(\underset{\sim}{H})\right| e^{i\psi(\underset{\sim}{H})} \qquad (8)$$

where $\psi(\underset{\sim}{H})$ is the phase difference between the diffracted and the incident beams. $|F(\underset{\sim}{H})|^2$ is related to the intensity of the diffracted rays for ideally mosaic crystals and can be experimentally determined. A complete knowledge of a diffraction phenomenon requires both $|F(\underset{\sim}{H})|$ and $\psi(\underset{\sim}{H})$ to be determined. However, currently available detectors are unable to make records of the phase angle $\psi(\underset{\sim}{H})$. In the current state of crystallography the determination of crystal structures centers around obtaining $\psi(\underset{\sim}{H})$ via indirect and statistical methods which are well summarized elsewhere.[2] These indirect methods are limited to certain applications and cannot be used for general crystallographic structure determination.

In order to determine the phase $\psi(\underset{\sim}{H})$, another X-ray beam coherent with the incident beam and propagating in the direction of the diffracted ray, TP may be used. Let $E(\underset{\sim}{H}) = F(\underset{\sim}{H})P(\underset{\sim}{H})$ where $P(\underset{\sim}{H})$ is a real function describing various crystallographic corrections including Lorentz and polarization factors. E(H) is the amplitude of the diffracted beam. Interference of the diffracted beam $E_1(\underset{\sim}{H})$ and the second beam $E_2(\underset{\sim}{H})$ will take place and the sum E_s contains the phase information. For the present let us ignore misalignments between the two coherent beams and assume that their wave fronts arrive simultaneously at T. The relative phase angle between $E_2(\underset{\sim}{O})$ and the diffracted beam $E_1(\underset{\sim}{H})$, $\varphi(\underset{\sim}{H})$, can be obtained by simple vector addition:

$$\cos \Psi(\underset{\sim}{H}) = \frac{|E_s|^2 - |E_1(\underset{\sim}{H})|^2 - |E_2(\underset{\sim}{O})|^2}{2|E_1(\underset{\sim}{H})||E_2(\underset{\sim}{O})|\cos\gamma_c} \qquad (9)$$

$|E_s|^2$ is the intensity when the two beams are present, while $E_1(H)^2$ and $E_2(O)^2$ are the intensities when the second beam is blocked and when the primary beam is blocked, respectively. $\cos \gamma_c$ is an additional correction factor for polarization effects since only beams of the same polarization state will interfere.

Although the method described above is workable, for every diffraction maxima $\underset{\sim}{H}$ we have to reset the intersection angle of the interfero-diffractometer, and hence cause a shift in the position of T in the diffracting crystal. Meaningful results can be extracted from Eq. (9) only when the bisecting plane of the two interferring rays maintains a constant spatial relationships with the crystal so that all the relative phases share one common origin. In order to monitor the stability of the system, we propose the following method of simultaneous diffraction. The geometry of diffraction is shown in Figure 4. The angle of intersection δ is chosen that upon entering the sphere of reflection, both ends of a selected reciprocal vector $\underset{\sim}{H}_o$ serve as origins of reciprocal lattices for the two rays I_1 and I_2. The crystal is rotated about an axis $\underset{\sim}{h}_o$ which is parallel to $\underset{\sim}{H}_o$, and both $\underset{\sim}{h}_o$ and $\underset{\sim}{H}_o$ are perpendicular to the bisecting plane of I_1 and I_2. The origin of the crystal lattice, T, is then defined as the intersection of $\underset{\sim}{h}_o$ and the bisecting plane of I_1 and I_2. As the crystal rotates about $\underset{\sim}{h}_o$, at a certain angle, a reciprocal lattice point P will pass

through the surface of the sphere of reflection defined by $\underset{\sim}{H}_o$, I_1 and I_2. Both I_1 and I_2 will be diffracted in the direction of TP, by two corresponding sets of planes $\underset{\sim}{H}_1$ and $\underset{\sim}{H}_2$ such that $\underset{\sim}{H}_1 - \underset{\sim}{H}_2 = \underset{\sim}{H}_o$. When both beams I_1 and I_2 are turned on, the two simultaneously diffracted rays in the direction of P will interfere, and phase determination can be carried out in the same manner as in Eq. (9).

As the crystal rotates, various other reciprocal points will appear on the surface of the Ewald sphere. For each such occurrence, the relative phase of the participating planes can be determined. A complete rotation will yield a whole set of phase relationships for reflections related by $\underset{\sim}{H}_o$. Since $\underset{\sim}{H}_o$ remains on the sphere of reflection for all $\underset{\sim}{H}_{AB}$'s with one setting of δ, $|E(\underset{\sim}{H}_o) + E(\underset{\sim}{Q})|^2$ can be used as a standard to monitor possible movement of the crystal origin as the crystal rotates about $\underset{\sim}{h}_o$.

The symmetry of the cosine function introduces an ambiguity in sign for the phase difference between each reflected pair; i.e., we cannot distinguish ψ from $2\pi - \psi$. However, if we collect two or more independent sets of phase relationships using independent $\underset{\sim}{H}_o$'s, we can cross correlate the phases. In general there will be only two sets of phases that satisfy all measured phase relationships, and these two sets of phases are once again related through a change of sign. However, if we use these two sets of phases in the Fourier summation, only one set will produce the true electron density map for the unknown crystal structure.

If we carefully choose three independent reciprocal vectors, e.g., the three principle reciprocal axes $\underset{\sim}{a}^*$, $\underset{\sim}{b}^*$, and $\underset{\sim}{c}^*$, and

independently collect three sets of phase relationships, then we can correlate the three sets and find the relative phases for all reflections.

In reality, statistical methods have been developed to such sophistication that only a small percentage of known phases will suffice to generate the rest due to the internal consistency of intensity data.

VI. Feasibility of Interfero-Diffractometer.

In order to satisfy the coherence conditions at the intersection point, the phases of the wave fronts of the two beams must be maintained to within a fraction of the wavelengths used; the accuracy of the determined value of the phase is 2π times the ratio of uncertainties in the position of the relative wave fronts to the wavelength. If a typical value of λ is 1.5 Å, in order to determine the phases to within 36^{o} it is necessary to maintain the wave front difference to within a linear dimension of 0.15 Å. The following problems are encountered in this consideration: (1) Maintainance of phase coherence in design, (2) Temperature and vibration effects, (3) Dimensional stability of materials, (4) Means of monitoring sub-Ångstrom dimensional changes as well as making corresponding corrections. In addition, one must consider (5) The adequacy of the intensity of the two interfering beams for a meaningful set of data within a reasonable amount of time.

(1) Maintainance of phase coherence in design. The central problem is the maintainance of phase coherence aftering passing through the path correction wedges LP (Figure 2). If we choose $\theta' = 49.9^{\circ}$ (Ge 440 plane at Cu K wavelength), $\theta = 22.5^{\circ}$ (Ge 220 plane), then the wedge angle η_0 is 36.8°. The chief purpose of the wedges is to compensate the path length so that the residual differences do not exceed the correlation length of the photon. The advantage of using the Borrmann effect to compensate the path lengths is the assurance of phase coherence of the exit beam, even though the surfaces are haggard on the atomic scale. Thus the requirement on the accuracy of the wedge angles is that the compensated path length at different locations across the beam is within the photon correlation length. If the actual wedge angle η departs from the calculated value η_0 from Eq. (2), a small residual source dependence of the path length, denoted by $d\Delta\ell$, will be present. The expression for $d\Delta\ell$ in terms of Δt, the position of the beam referring to the central value, t, is

$$d\Delta\ell = -\frac{2(1-\cos\theta')}{\cos\theta'} \sec^2\eta_0 \cos\theta \cdot \Delta t(\eta-\eta_0) \qquad (10)$$

Numerically, using the examples of Section II (iii), i.e., $\eta_0 = 36.8^{\circ}$, $\theta = 22.5^{\circ}$, $\theta' = 49.9^{\circ}$, then

$$d\Delta\ell = -1.6\,\Delta t\,\Delta\eta \qquad (11)$$

Take for example, $\Delta t = 0.5$ mm $= 500\,\mu$, and let us assume that the allowable error in $d\Delta\ell$ is $5\,\mu$ (around 1/10 of the photon

correlation length), then the maximum allowable error $(\eta - \eta_o)$, is around 1/160 radians or around 20 minutes of arc.

The use of the two Borrmann transmission wedges to compensate the source position dependence of the path lengths will introduce a source position dependence in the beam intensity. To correct for this, two additional wedges A_1 and A_2 are inserted into the path of the beam I_2, as shown in Figure 5. Both A_1 and A_2 are made of amorphous materials so that there is no diffraction effect. A_1 is made of a highly absorptive material in the wave length regions of interest, while A_2 is made of a highly transparent material. The function of A_1 is to correct for the source position dependence of the intensity of the beam, and that of A_2 is to correct for the source position dependence of the phase lag of the beam after transmission through A_1.

Transmissions through the wedge via the Borrmann effect will introduce a position dpenedent absorption factor

$$\exp -\mu_o(1 - \epsilon)\ 2 \sin \theta\ dt$$

where dt is the distance measured with respect to the extremity of the beam where the intensity is greatest, in the direction perpendicular to the beam. (Figure 5.) If the thickness of A_1 and A_2 are described by two functions $S_1(dt)$ and $S_2(dt)$ respectively, their mass absorption coefficients μ_1 and μ_2 respectively, then the additional absorption factors associated with A_1 and A_2 are $\exp - \mu_1 S_1(dt)$ and $\exp - \mu_2 S_2(dt)$ respectively. In order that the position dependence of the intensity be eliminated, it is necessary

that the combined absorption factor remain a constant independent of dt:

$$\exp -\mu_0(1-\epsilon)2\sin\theta\, dt \cdot \exp -\mu_1 S_1(dt) \cdot \exp -\mu_2 S_2(dt) = \text{const.}$$

which leads to the equation:

$$\mu_1 S_1(dt) + \mu_2 S_2(dt) + \mu_0(1-\epsilon)2\sin\theta\, dt = \text{const.} \qquad (12)$$

In passing through A_1 and A_2, soruce dependent phase lags due to differences in the thickness of A_1 and A_2 will result. At wavelengths far away from absorption edges, the index of refraction n is given by:

$$n = 1 - \frac{\Omega^2}{\omega^2} \qquad (13)$$

where $\Omega^2 = \frac{4\pi n e^2}{m}$, N is the average electron density. A phase lag $\delta_i(dt)$ is introduced at dt such that:

$$\delta_i(dt) = \frac{S_i(dt)}{\lambda} \frac{\Omega^2}{4\pi\omega} \qquad (14)$$

where i = 1,2 for A_1 and A_2 respectively. The condition for a constant phase lag is then:

$$\delta_1(dt) + \delta_2(dt) = \left[S_1(dt)\Omega_1^2 + S_2(dt)\Omega_2^2\right]\frac{1}{4\pi\lambda\omega} = \text{Constant} \qquad (15)$$

Eqs. (12) and (15) determines $S_1(dt)$ and $S_2(dt)$ uniquely as functions of dt. The solution is

$$S_1(dt) = C_1 - \frac{\mu_0}{\mu_1 - \mu_2 \frac{N_1}{N_2}} (1-\epsilon) 2 \sin\theta dt \qquad (16)$$

$$S_2(dt) = C_2 - \frac{\mu_0}{\mu_2 - \mu_1 \frac{N_2}{N_1}} (1-\epsilon) 2 \sin\theta dt \qquad (17)$$

If we choose $\mu_1 = \mu_0$, $\mu_2 = 0$, $N_1 = N_2$, then

$$S_1(dt) = C_1 - (1-\epsilon) 2 \sin\theta dt \qquad (18)$$

$$S_2(dt) = C_2 + (1-\epsilon) 2 \sin\theta dt \qquad (19)$$

Using the parameters quoted previously, i.e., $1-\epsilon = 0.05$ $dt_{max} = 0.5$ mm the variations of S_1 and S_2 are roughly 25 μ across the beam. The total phase lag introduced is less than 2π (See Eq. (13)). This means that a 1 % error in the fabricated thickness of corrector plates for intensity and phase lag is sufficient to insure that a 1 % accuracy in the phase angle can be achieved.

(2) Temperature and vibrational effects.

Most materials have thermal expansion coefficients ϵ_{th} in the range 10^{-6} - 10^{-8}. If the path difference of the two beams is $\Delta\ell$, then $\Delta\ell$ varies with temperature as $\Delta\ell\,\epsilon_{th}\Delta T$ where ΔT is the temperature fluctuation. If $\Delta\lambda = 10\,\mu$ (10^{-3} cm), ($\Delta\ell$ must be less than the photon correlation length), then with $\epsilon_{th} = 10^{-7}$, a temperature variation of 10°C will give rise to a path length variation of 10^{-9} cm = 0.1 Å. On the other hand, differential temperature conditions of value ΔT_ℓ along the two beam

paths will give rise to an additional thermal term $\ell \epsilon_{th} \Delta T_d$. With ℓ = 10 cm, $\epsilon = 10^{-7}$, in order to keep the path length differences to below 0.1 Å, it is necessary that any differential temperature be kept below 10^{-3} °C . A number of low thermal expansion materials have been developed for precision optics.[10] The thermal expansion coefficient of some of these materials changes sign at a certain temperature (zero expansion temperature), so that thermal expansion vanishes.. These materials include ULE (a nonmetal) and superinvar (a metal). Their thermal expansion coefficients vanish at around 45° C (Figure 6). These materials can be used for the construction of the interfero-diffractometer. Other similar types of low thermal expansion materials also exist with somewhat different zero expansion temperatures.

The completed instrument will have a dimension of a few ten's of centimeters. The natural resonance frequency will be of the order of a few hundred to a few thousand hertz. Well established methods of vibration isolation can be used to remove these frequencies. Sub-hertz vibrations will not affect the dimensional stability severely.

(3) Dimensional stability of materials. Internal stress will cause most materials to exhibit temporal variations in dimensions. In a series of experiments, Jacobs and his associates made a fairly thorough study of the dimensional stability of a number of materials over a time interval of several months.[11] Their results are summarized in Figures 7 and 8. The initial variations in dimensions are probably caused by the settling of optical contact surfaces of the monitoring components, and probably do not represent real changes in dimensions.[12] As seen in Figures 7 and 8, the two materials

ULE and superinvar exhibit the best dimensional stability properties.

(4). Techniques for measurement of sub-Ångstrom dimensional changes have been developed for various purposes, including studies (2) and (3). The principle used in one of the measuring techniques is as follows: A stable laser of frequency ν_0 is tuned to frequencies $\nu_1 = \nu_0 + \Delta\nu$, $\nu_2 = \nu_0 - \Delta\nu$ by mixing the laser radiation with a microwave source of frequency $\Delta\nu$ in an optically nonlinear medium. One of the two tuned frequencies say, $\nu_1 = \nu_0 + \Delta\nu$, is introduced into an optical cavity of length ℓ which is to be measured. The value of $\Delta\nu$ is adjusted for the maximum transmission peak, which in the current stage of technology, can be made to have a full width at half maximum of less than 5 MHz.[11] By monitoring the value of $\Delta\nu$, to say, 10^5 Hz, (1/50 of the transmission width)), it is possible to achieve an accuracy in $d(\Delta\nu/\nu_0)$ to one part in 10^{11}. This corresponds to an accuracy in dimension measurement of $d\ell/\ell$ to 10^{-11}. By using two optical cavities of different optical lengths but of reflective coatings prepared at the same time, the effects of time variations of phases in reflections can be minimized. Currently available stable lasers exhibit a frequency stability of better than one part in 10^{11}.[13] Techniques for measurements of dimensions to accuracies of 10^{-3} Å have also been developed.[14]

(5) Intensity. Although the intensity of raw radiation from a conventional X-ray generator is farily high, its angular divergence as well as its bandwidth is large. After transmission through crystal planes via the Borrmann effect, the angular divergence of the exit beam is narrowed to a few seconds of arc, and the bandwidth is also reduced to below 10^{-5}, resulting in a drastic reduction in intensity. In our proposed set up, further reductions in intensity will result from transmissions through and reflections by crystal planes in the path correction wedges.

An estimate of the intensity of the two interfering beams will now be given. According to Cole et al[15], a conventional X-ray generator operating at 35 kV and at 16 mA beam current, after passing through a perfect crystal of thickness of 1 mm via the Borrmann effect, yields a pair of splitted beams (λ = 1.54 Å) each with a total intensity of 5,000 counts per second over a cross-sectional area of 1 mm x 1 mm. Let us assume that the cross-sectional area of the beam in our case to be 0.5 mm (width) x 1 mm (height). We now use Cole's value for the intensitities of I_1 and I_2 at the beam splitting point in Figure 2. In our setup, I_1 passes through two additional reflections, at LP and M_1. If the surface of LP and M_1 are parallel to the reflecting crystalline planes, the reflectivity is in the neighbourhood of 0.9, and the intensity of I_1 at the intersection point T is $0.9 \times 0.9 \times 2.5 \times 10^3 = 2 \times 10^3$ count/sec.

The intensity of I_2 will suffer a much higher attenuation. There are three sources of attenuations: (a) through reflections in the multiple reflection path extender, (b) through transmissions in the path correction wedges, (c) through reflections in M_2. In

the case of (a), the attenuation factor of a twice reflected path extender will give an attenuation factor of 0.8. Assuming that the thickness of the wedge at the narrowest path of the wedge to be 0.5 mm, then in (b) an additional attenuation factor for the two wedges is $\exp -\mu_o(1-\epsilon)t = 0.17$. The additional factor in (c) is 0.9. The overall attenuation factor is then $0.17 \times 0.9 \times 0.8 \times 0.25 = 3 \times 10^{-2}$. The last factor of 0.25 arises from the worst case of source dependence of the beam. The intensity of I_2 at T is then 150 count per second. (In practice, further attenuations due to departures from the minimum geometry configurations we discussed will occur.)

Assuming that the diffracted intensity from the sample crystal to be 10^{-5} of the incident beam, the intensity of the diffracted beam from I_2 (the weaker beam) is 1.5×10^{-3} / sec, or 130/ day. The associated signal to noise ratio is 11. If the phase angle is around 45^{o}, the corresponding error in the determined phase, according to Eq. (9), is in the neighbourhood of tens of degrees.

Naturally this estimate may be somewhat optimistic. What we have shown is that, the intensity from a conventional X-ray generator will not yield a truly unrealistic counting rate (e.g. 100 count in a year). A more intense source such as rotating anode generator will increase data collection rate by roughly 5 times. A new source of X-ray radiation is the synchrotron radiation which offers an advantage over conventional X-ray generators by a factor of 2,000 to 50,000. The determination of phases can then be achieved within half an hour for a single measurement, provided that area detectors with single quantum detection capability are used. Area detectors with single quantum detection

capability are within the realm of feasibility.

V. Conclusions.

In this paper we have presented a scheme to measure the relative phases of diffracted X-rays. Although the requirement in dimensional stability and intensity of X-ray sources is demanding, we have shown that such requirements are within the realm of technological feasibility. Due to the nature of the problem, it is our opinion that even with the successful development of an X-ray laser as a source of coherent X-rays, an interfero-diffractometer of the type described in this paper must be used to split the incident beam and recombine it to produce interference in the diffracted rays from mosaic crystals, with the possible absence of the beam path correction wedge crystal due to the long coherence length associated with laser radiations. The lack of a proper recording medium with resolution in the sub-Ångstrom range prevents the use of holographic techniques to probe molecular structures in the atomic level, with X-ray lasers.

VI. Acknowledgements.

We would like to thank Drs. B. W. Batterman, H. Bernstein, H. Berman, B. M. Fairchild, E. Hoff, B. Post and E. E. Salpeter for discussions, and Dr. S. P. Maran for reading the manuscript for editorial corrections.

References

1. In certain special n-beam cases, phase information has been extracted from coherent beams generated within the specimen (Post, B., private communication and to be published). These studies contribute significant insight to the dynamical theory of X-ray diffraction. However, the stringent requirements in regards to the establishment of an n-beam case limit it to special cases rather than to structure determination in general.
2. Hauptman, H., and Karle, J. "Solution of the Phase Problem I. The Centrosymmetric Crystal", ACA monograph No. 3, Pittsburgh: Polycrystal Book Service (1953). Hauptman, H., Acta Cryst. 30, 822 (1974), Karle J. and Karle, I.L., Acta. Cryst. 21, 849 (1966), Woolfson, M., Acta. Cryst. B26, 274 (1970), A27, 368 (1971), Carlisle, C. H., and Crowfool, D., Proc. Roy. Soc. A184, 64 (1964), Okaya, Y. and Pepinsky, R., Phys. Rev. 103, 1645 (1956), Perutz, M. F., Acta. Cryst. 9, 867 (1956), Kendrew, J. C., Nature 181, 662 (1958), Bodo, G., Dintris, H. M., Kendrew, J. C., Wyckoff, H. W., Proc. Roy. Soc. A253, 70 (1959), Germain, G. and Woolson, M. M., Acta. Cryst. B24, 91 (1968), Germain, G., Main, P. and Woolson, M. M., Acta. Cryst. B26, 274 (1970), A27, 368 (1971), Berman, H. M., Acta. Cryst. B26, 290 (1970).
3. Bonse, U. and Hart, M. Applied Phys. Lett., 6, 155 (1965), Z. Physik, 188, 154 (1965), 190, 455 (1966), 194, 1, 455 (1966).
4. Werner, S. A., Colella, R., Overhauser, A. W., and Eagen, C. F., Phys. Rev. Letters 35, 1053 (1975).

6. Chiu, C. C., Sunny Technical Report, No. 4 (1976).

7. Bonse, U. and Hart, M., Acta. Cryst. A24, 240 (1968), Z. Physik, 214, 16 (1968).

8, Parak, F., Mössbauer, R. L., Biebl, U. Formanek, H., and Hoppe, W., Z. Physik, 244, 456 (1971). With a 0.05 Curie source, the beam width is 2 mm x 2 mm and the counting rate in a certain Bragg diffraction direction is around one per minute.

9. Robinson, A. L., Science, 190, 1074 (1975).

10. Jacobs, S. F., Berthold III, J. W., Norton, M. "Measurement of Dimensional Stability", Final report under NASA contract NAS 8-28661.

11. Jacobs, S. F., Bradford, J. N., and Berthold III, J. W., Applied Optics 9 2477 (1970).

12. Jacobs, S. F. (Private communication).

13. Many types of stable lasers have been developed. See for example, Barger, R. L., and Hall, J. L., Phys. Rev. Letters, 22, 4 (1969).

14. Boersch, J., Eichler, H. and Wiesemann, W., Appl. Opt. 9, 645 (1970).

15. Cole, H., Chambers, F. W., and Wood, C. G., Journal of Applied Physics, 32, 1942 (1961).

Figure Captions

Figure 1. Borrmann effect. An incident beam at Bragg angle θ_o with the set of planes LP sets up wave fields and propagates along LP in the beam splitter crystal BS. At the exit surface the wave field is split into two beams TR and FD which propagate in two separate directions, with an angular separation of 2 θ_o. The direct transmitted beam DT is suppressed by normal absorption.

Figure 2. Schematic diagram of an interfero-diffractometer.

Figure 3. Geometry of diffraction.

Figure 4. Geometry of simultaneous diffractions of two coherent beams into a common direction.

Figure 5. Correction plates for intensity and phase lag.

Figure 6. Thermal expansion coefficients for a number of commercially available materials noted for low thermal expansion. From Reference 11.

Figure 7. Dimensional stability of ULE. The ordinate is the tuning frequency that is necessary to satisfy the maximum transmission condition of the associated optical cavity. Generally the fractional dimensional change is the same as $d\Delta\nu/\nu_o$ where ν_o is the laser frequency and is in the range of 10^{16}. $d\Delta\nu$ is the change of $\Delta\nu$ in the course of investigation. From reference 10.

Figure 8. Dimensional stability of superinvar. See Figure 7 for detailed explanations. From reference 10.

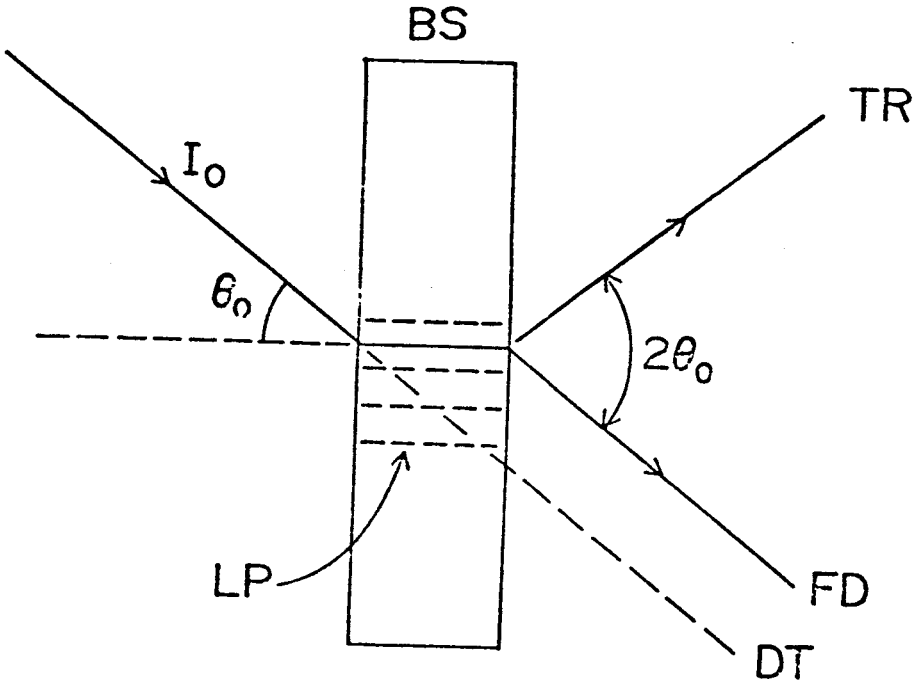

Figure I - Borrmann effect

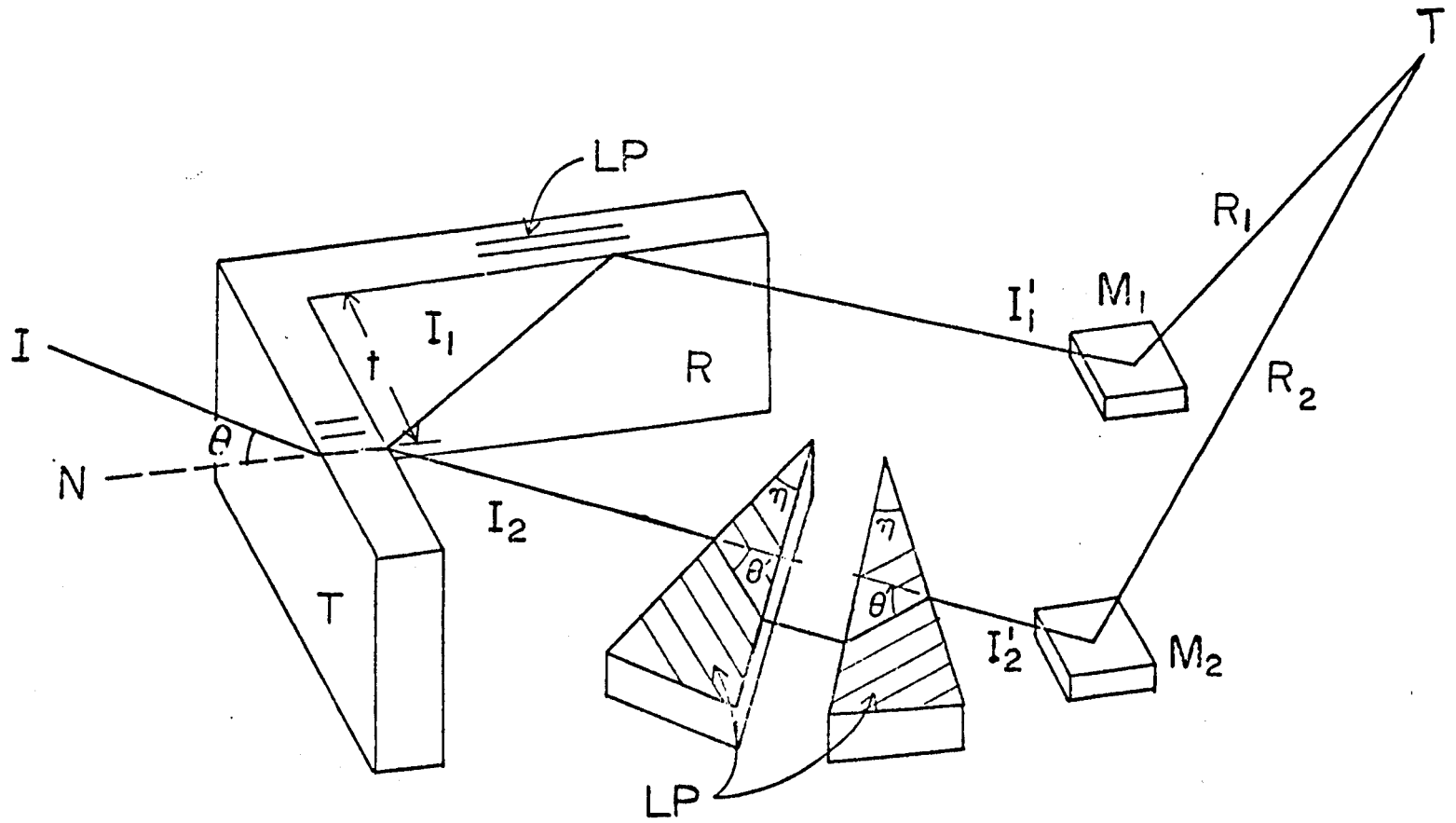

Figure 2- Interfero-diffractometer Configration

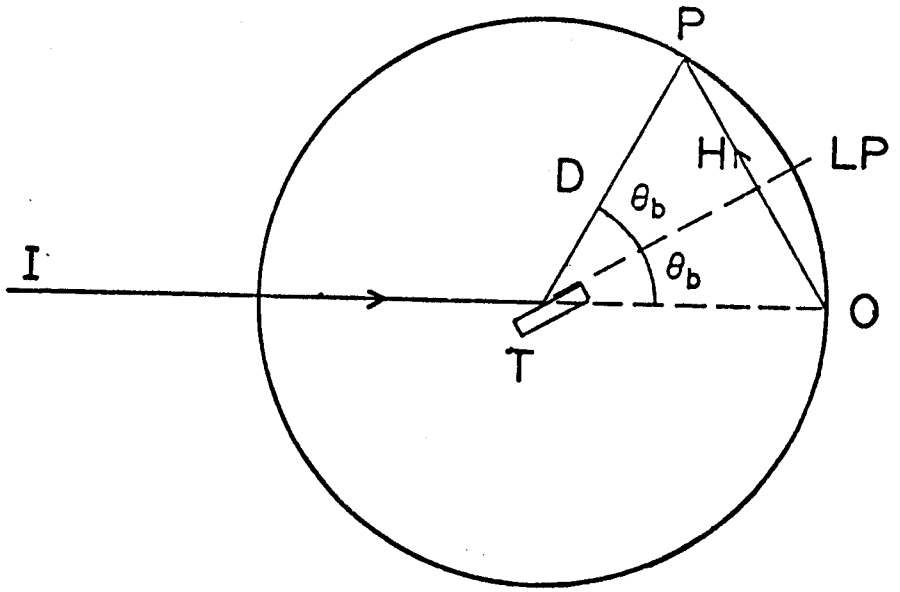

Figure 3

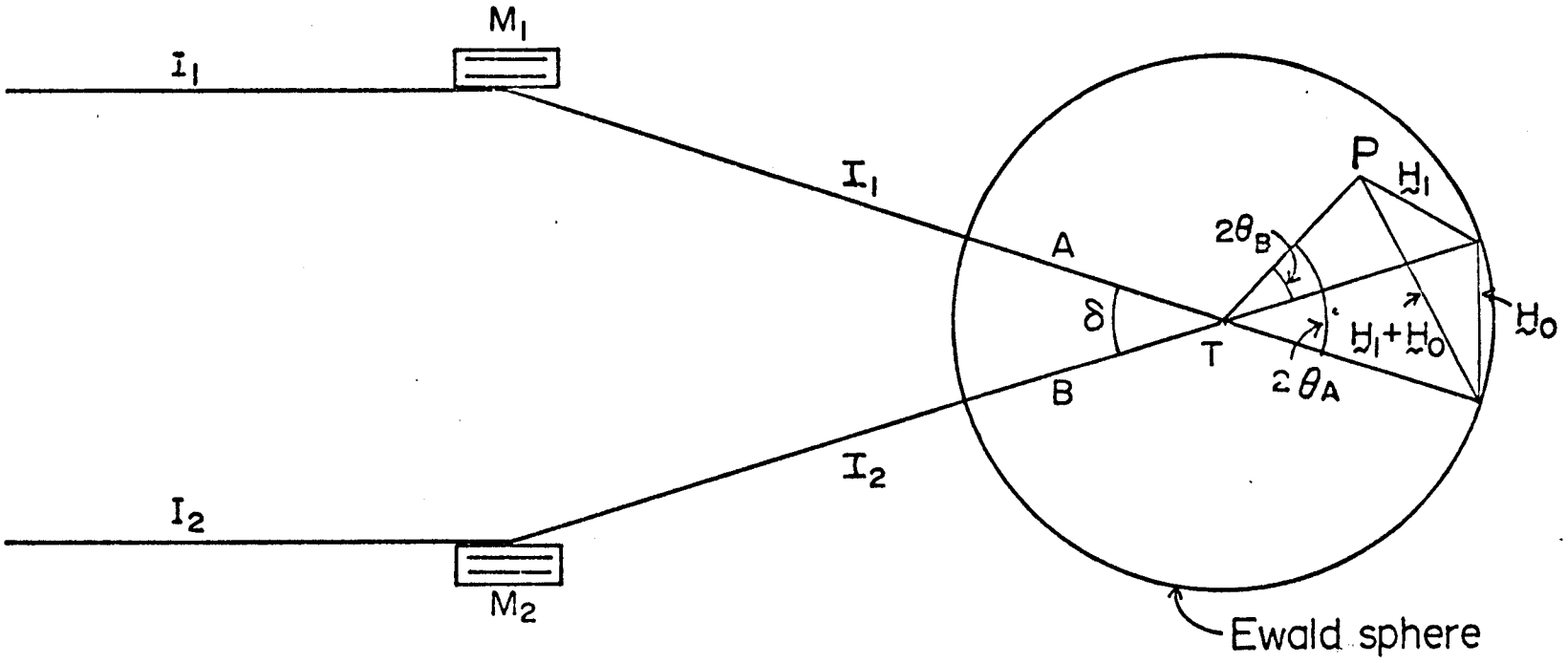

Figure 4

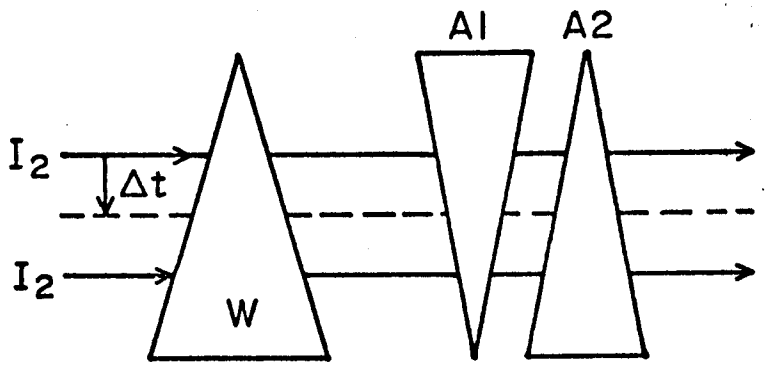
A1
A2
I_2
Δt
I_2
W

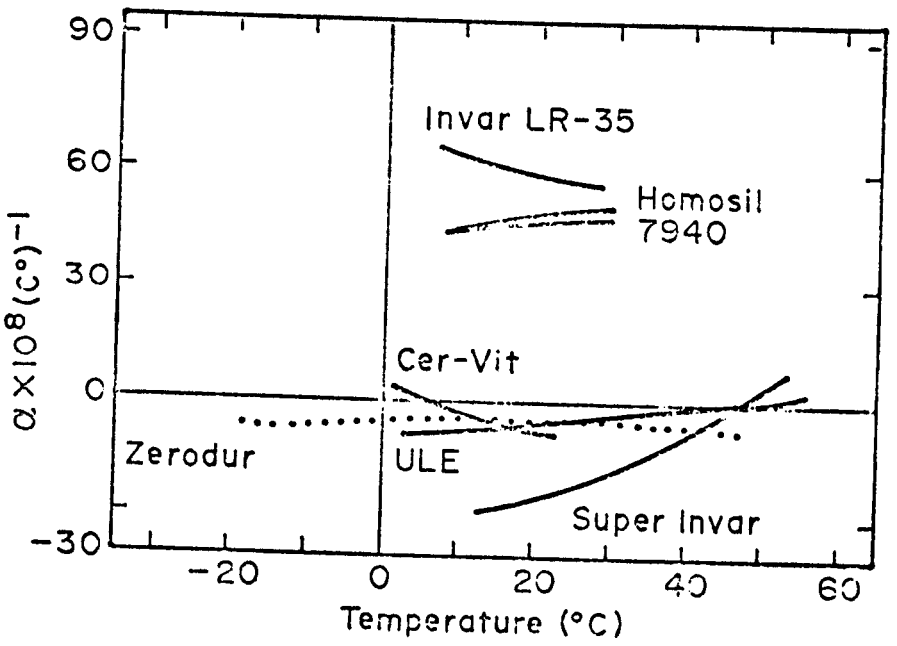
90
60
30
0
-30
$\alpha \times 10^8 (C°)^{-1}$
Invar LR-35
Homosil
7940
Cer-Vit
Zerodur
ULE
Super Invar
-20
0
20
40
60
Temperature (°C)

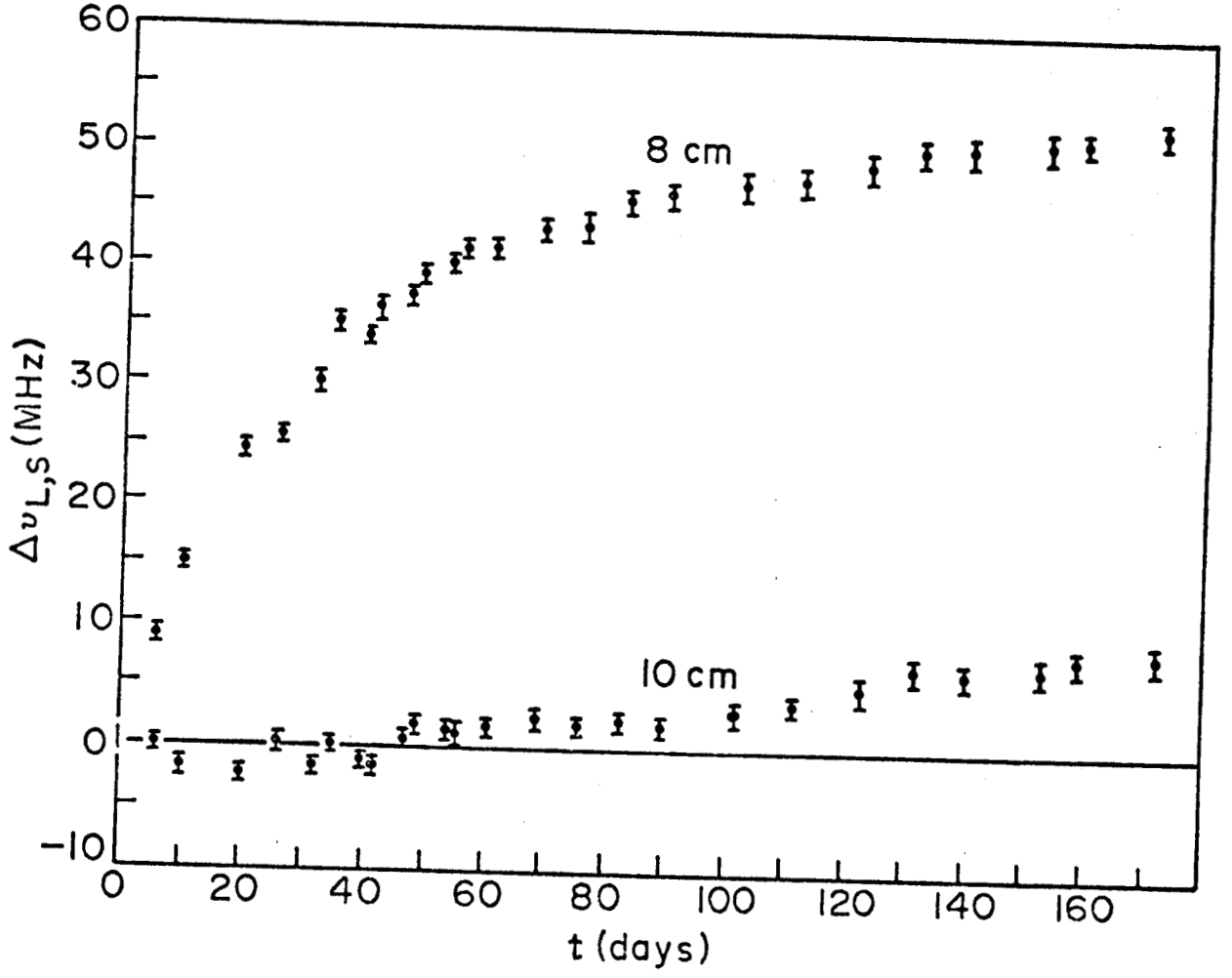
60
50
40
30
20
10
0
-10
$\Delta\nu_{L,S}$ (MHz)
8 cm
10 cm
0
20
40
60
80
100
120
140
160
t (days)

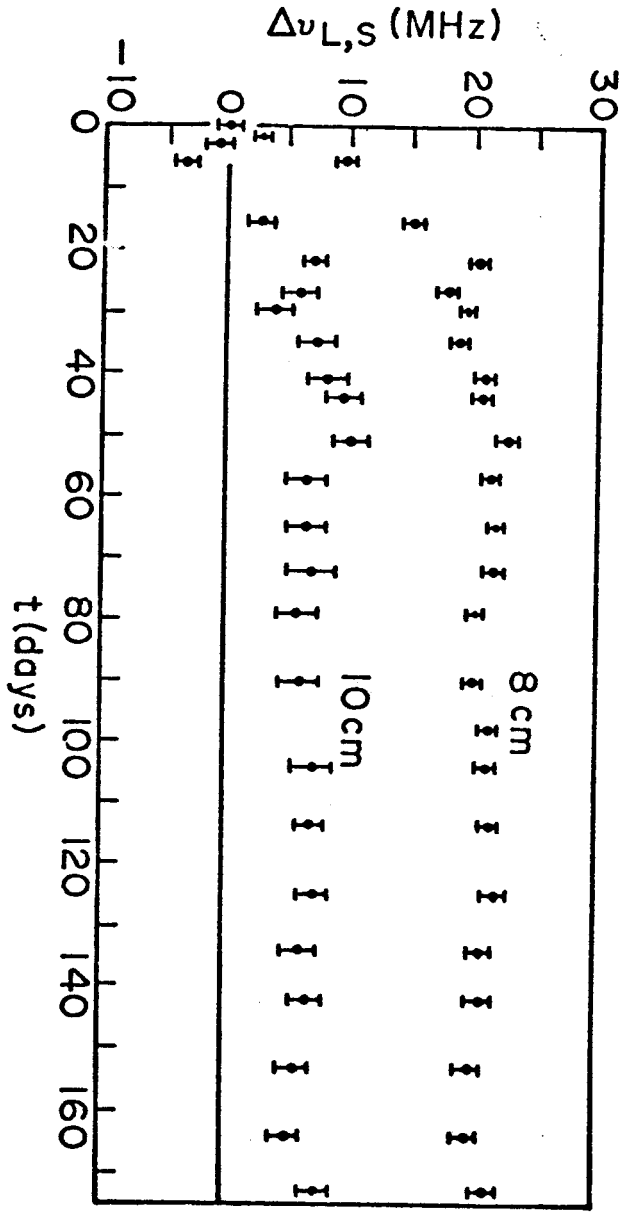
$\Delta\nu_{L,S}$ (MHz)
-10
0
10
20
30
0
20
40
60
80
100
120
140
160
t (days)
10 cm
8 cm